www.czasopisma.pan.pl PAN POLSKA AKADEMIA NAUK www.journals.pan.pl

ARCHIVES OF ACOUSTICS Vol. 48, No. 1, pp. 63–70 (2023), doi: 10.24425/aoa.2022.142907

Research Paper

Improvement of Sound Insulation Through Double-Panel Structure by Using Hybrid Local Resonator Array

Kyong-Su RI, Myong-Jin KIM*, Se-Hyon SON-U

Institute of Acoustics, Department of Physics, Kim Il Sung University
Pyongyang, Democratic People's Republic of Korea

*Corresponding Author e-mail: mj.kim0903@ryongnamsan.edu.kp

(*received March 5, 2021; accepted September 2, 2022*)

In this paper, we present one approach to improve the soundproofing performance of the double-panel structure (DPS) in the entire audible frequencies, in which two kinds of local resonances, the breathing-type resonance and the Helmholtz resonance, are combined. The thin ring resonator row and slit-type resonator (Helmholtz resonator) row are inserted between two panels of DPS together. Overlapping of the band gaps due to the individual resonances gives a wide and high band gap of sound transmission in the low frequency range. At the same time, the Bragg-type band gap is created by the structural periodicity of the scatterers in the high audible frequency range. In addition, the number of scatterer rows and the filling factor are investigated with regard to the sound insulation of DPS with sonic crystals (SCs). Consequently, the hybrid SC has the potential of increasing the soundproofing performance of DPS in the audible frequency range above 1 kHz by about 15 dB on average compared to DPS filled only with glass wool between two panels, while decreasing the total thickness and mass compared to the counterparts with the other type of local resonant sonic crystal.

Keywords: sound insulation; local resonance; insertion loss; sonic crystal.

1. Introduction

BRILLOUIN (1946) described mathematically the propagation of waves in periodic structures in 1946. Subsequently, the transmission properties of the electromagnetic wave in periodic structures was studied in late 1980s. It was shown that infinite periodic structures do not support wave propagation in certain frequency ranges relating to the spacing between the scattering elements (Lattice constant).

The first experimental study on the sound attenuation by periodic structure was undertaken in 1995 (MARTÍNEZ-SALA *et al.*, 1995). The sculpture consists of a periodic square symmetry arrangement of stainless steel pipe with a diameter of 29 mm, a distance between 2 pipes next to each other of 100 mm. Filling factor of 0.066 was used in their experiment. Sound attenuation was measured at various angles in outdoor conditions for sound wave incidences perpendicular to the cylinders' vertical axes, resulting in several maxima (sound attenuation) and minima (sound reinforcement) in the frequency spectrum. The first (lowest) band gap had a center frequency at 1.7 KHz, which could be attributed to the periodicity of the structure. Ever since, researches on the application of periodic arrays of cylinders for noise control have increased (SANCHEZ-PEREZ *et al.*, 2002; ROMERO-GARCÍA *et al.*, 2011). Investigation of sound attenuation effects of regularly planted trees has also been conducted (MARTÍNES-SALA *et al.*, 2006). There were numerical and theoretical works in respect to periodic arrays of elastic scatterers in gas involving hollow spheres and cylinders (SAINIDOU *et al.*, 2006).

Local sound absorption properties have been used in sonic crystal noise barriers. For example, both numerical and experimental studies have been made of the reflectance and transmittance spectra of the sonic crystals (SCs) consisted of rigid perforated cylindrical shells filled with recycled rubber crumb material (SÁNCHEZ-DEHESA *et al.*, 2011). Such design offers the additional mechanism of absorption, apart from the multiple scattering phenomenon in periodic structure, to further attenuate noise (UMNOVA *et al.*, 2006).

A conventional way for reducing low frequency noise transmission is to increase the thickness or mass per unit area of the sound insulation material. However, a drawback of this technique is that usually it results in large size and mass of the insulator. One possibility for targeting the band gap without increasing the size is to use the resonant scatterers. Besides Helmholtz resonator, there are several cavity-type resonators such as half- and quarter-wave tubes, which are used comonly on air intake systems to attenuate noise at specific frequencies (Sohn, Park, 2011).

The concept of split ring resonator (SRR) was initially introduced in 1999 in the electromagnetism field. There have been theoretical and experimental studies on SRR which gave the frequency range related to the resonant frequency in which waves could not propagate through the system (Movchan, Guenneau, 2004; Wu *et al.*, 2008). Another type of SC using concentrically placed Helmholtz resonators has been studied numerically (Elford *et al.*, 2011). It was found that the natural resonance properties of the six shell Matryoshka SC give rise to multiple independent resonance band gaps below the first Bragg band gap (i.e., due to the periodicity of the SC) between 400 and 1600 Hz. There have also been numerical studies of acoustical performance of a periodic array of resonant silicone rubber scatterers embedded in an epoxy resin matrix (Hirsekorn *et al.*, 2004). Experimental work in respect to periodic array of scatterers in air has investigated the use of pressurized gas-filled cylindrical balloons (Fuster-Garcia *et al.*, 2007). It was found that resonance attenuation peaks can be obtained at frequencies which do not depend on the periodicity of the SC but on the resonance frequency of the resonators. Predictions and measurements of sound transmission through a periodic array of elastic shells in air have been conducted (Kyrnkin *et al.*, 2010). Besides, several shapes of local resonant SCs have been proposed for enhancing the sound insulation through the multi-layer structures in the entire audible frequency range as well as in the low frequencies (Cavalieri *et al.*, 2019; Gulia, Gupta, 2018; 2019; Kim, 2019; Kim *et al.*, 2021; Qian, 2018).

Plane wave expansion (PWE) method is one of the most studied methods for research into the phononic or sonic crystal band gaps (Chen, Ye, 2001; Vasseur *et al.*, 2008). It can be applied to the infinite arrays of any scatterer shape. Multiple scattering approach was first published for the potential flow through a periodic rectangular array of identical cylinders in 1892. Subsequently, investigations on multiple scattering have been made for a variety of 2D or 3D problems (Linton, Evans, 1990).

Those two methods are not always feasible to solve for scatterers with non-geometrical shapes or resonant constructions by means of an exact analytical solution. In such a case, the finite element method (FEM) based on numerical solutions of partial differential equations (PDEs) offers a method for finding approximate numerical solutions of the scattered and total fields in a wide range of physical and engineering problems. The numerical results for the acoustical properties of SCs have been reported using the FEM commercial software such as COMSOL or ANSYS.

In this paper a DPS is proposed with a local resonant SC based upon the combination of the breathing resonance of a thin ring-type shell and Helmholtz resonance, and some issues for its application are also explored.

2. Numerical modelling

Figure 1 shows the schematic of DPS with SC as well as the Brillouin zone, which depicts the ΓX and ΓM directions of acoustic wave propagation. The SC consists of $7 \times n$ square arrangement of scatterers. Two panels of DPS have thickness of 4 mm and 6 mm, respectively, and are assumed to be made of plastic of which density, Young's modulus, and Poisson's ratio are 1380 kg/m^3, 3.2 GPa, and 0.37, respectively. The space between two panels changes with the number of scatterer rows. The domain between two panels is filled with air or porous material, glass wool. Density and sound speed of air are 1.2 kg/m^3 and 344 m/s, respectively.

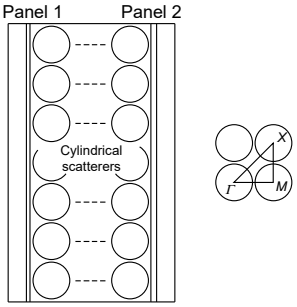

Fig. 1. DPS with $7 \times n$ square arrangement of scatterers and Brillouin Zone.

A plane wave source is applied to the entrance of DPS, i.e., the inward normal velocity is applied to the left boundary surface of the DPS in Fig. 1, while the infinite radiation conditions to the source and receiver boundaries. It can be assumed that there exists no back reflection of acoustic waves on such boundaries, and thus the following boundary conditions are satisfied (Gulia, Gupta, 2018b):

$$\left(-\frac{\nabla p}{\rho}\right) \cdot \mathbf{n} = \frac{i\omega}{\rho c_c} p - \frac{i\omega}{\rho c_c} p_0, \tag{1}$$

$$\left(-\frac{\nabla p}{\rho}\right) \cdot \mathbf{n} = \frac{i\omega}{\rho c_c} p, \tag{2}$$

where $p = p_0 e^{i\mathbf{kr}}$ and p is the acoustic pressure, $\mathbf{k}$ is the wave vector, ρ is the density, $\mathbf{n}$ is the normal vector,

ω is the angular frequency, and c_c is the sound speed. The surfaces of scatterers are assumed to be free to take account of the vibration of thin shells. The other boundaries of DPS are all considered to be solid wall. The normal particle velocity is equal to zero on the solid wall, where the Neumann boundary condition is satisfied as follows:

$$\left(-\frac{\nabla p}{\rho}\right)\cdot \mathbf{n} = 0. \tag{3}$$

In this work, glass wool is taken as porous material and modelled by Delay-Bazley model (Delany, Bazley, 1970). The wave number k_g and the characteristic impedance z_g of glass wool are then expressed by the complex forms:

$$k_g = \frac{\omega}{c_0}\left[1 + 0.0978\chi^{-0.7} - j0.189\chi^{-0.595}\right], \tag{4}$$

$$z_g = \rho_0 c_0\left[1 + 0.0571\chi^{-0.754} - j0.087\chi^{-0.732}\right], \tag{5}$$

where $\chi = \rho_0 f/R_g$, ρ_0 and c_0 are the density of fluid and the sound velocity in fluid without porous material, respectively, f denotes the frequency, ω indicates the angular frequency, and R_g marks the flow resistance of glass wool.

The mean fiber diameter (d_g) and density (ρ_g) are 10 μm and 12 kg/m^3, respectively. The flow resistance can be calculated by the expression as following (Bies, Hansen, 1980):

$$R_g = \frac{3.18\cdot 10^{-9}\rho_g^{1.53}}{d_g^2}. \tag{6}$$

SC is a periodic array of the finite scatterers embedded in homogeneous medium and can be characterized by the geometry of its primitive cell as in semiconductor. The concept of wave reflection in Bragg's Law which refers mainly to light diffraction can be analogously used for sound waves. In the periodic structures comprised of rigid scatterers, the sound waves could interfere with each other constructively and destructively, resulting in a total reflection regime (complete band gap) in certain frequency range. The frequency range depends on the lattice constant of the array as given by Bragg's Law. In a square lattice, the fundamental Bragg resonance frequencies in the ΓX and ΓM directions are, therefore, as follows:

$$f_{\Gamma X} = \frac{c}{2L}, \tag{7}$$

$$f_{\Gamma M} = \frac{c}{\sqrt{2}\,(2L)}, \tag{8}$$

where c is the sound speed in host medium. If the two Bragg resonances are wide enough in frequency to overlap, then a complete band gap can be realized based solely on the Bragg resonance condition. The width and depth of Bragg resonance is dependent on the acoustic impedance mismatch between the host medium and scatterer as well as the filling fraction (function of lattice constant). Forming a sonic band gap requires the careful selection of materials with both the mass densities and modulus to yield the desired acoustic impedance, and velocity mismatch between the matrix and scatterer.

The resonant frequency of SRR is given by Chalmers *et al.* (2009):

$$f = \frac{c}{2\pi}\sqrt{\frac{\sigma}{S\left\{L + \frac{1}{2}\sqrt{\pi\sigma}\right\}}}, \tag{9}$$

where L is the neck length, σ is the slit width, and S is the inner cross-sectional area. It can be seen that the Helmholtz resonance frequency decreases with increasing the volume of the air cavity and the length of the neck while increases with increasing the slit width.

Calculations are conducted in the FE software ANSYS Multiphysics (v18.0) acoustic package and the soundproofing performances of DPSs are evaluated through the sound transmission loss (STL) and insertion loss (IL), assuming that the flanking sound transmission is negligibly small.

If the power incident on the DPS (left side in Fig. 1) is W_i and the power transmitted through the DPS (right side in Fig. 1) is W_t, STL is determined by:

$$\mathrm{STL} = 10\log\left(\frac{W_i}{W_t}\right). \tag{10}$$

IL is calculated from the following equation:

$$\mathrm{IL} = 10\log\left(\frac{W}{W'}\right), \tag{11}$$

where W and W' refer to the power transmitted through the DPS without or with the scatterer array.

Harmonic analysis is performed in the range of 20–8000 Hz with the frequency interval of 20 Hz. The model is meshed with an element size (about 4 mm) of one-tenth of the minimum wavelength.

3. Results and discussion

3.1. Number of scatterer rows and filling fraction in DPS

The filling fraction is defined as the ratio between the volume occupied by one scatterer and the volume occupied by a unit cell and thus can be determined once the lattice constant and the size of the scatterers are known. Properly specifying the number of scatterer rows and the filling fraction is very important for decreasing the geometrical size and cost of DPS. For this purpose, the Bragg band gap was investigated with varying such two parameters by the finite element method.

The shapes of scatterers are cylindrical and they are arranged on $7 \times n$ square lattice as in Fig. 1. The cylinders have an outer diameter of 40 mm and the lattice constant of SC is 42.8 mm. The number of rows, n, is varied from 1 to 3. The domains between two panels and scatterers are considered to be filled with air.

Figure 2 shows the IL spectra as a function of the number of scatterer rows. For all three cases, there is a peak of IL around 4020–4040 Hz, which matches well with the Bragg frequency calculated by Eq. (7) for the lattice constant of 42.8 mm. Bragg band gap cannot be created for one row of scatterers in free space. However, DPS with one row of scatterers gives a distinct band gap around the Bragg frequency due to the multiple reciprocating reflection between two panels. The ILs at the Bragg frequency are 49.7 dB, 56.9 dB, and 64.8 dB for the number of rows from 1 to 3, respectively. For the number of 2 and 3, several sharp peaks appear in the insertion loss spectrum, which might be attributed to the suppression of stand wave resonance by the inserted array of scatterers.

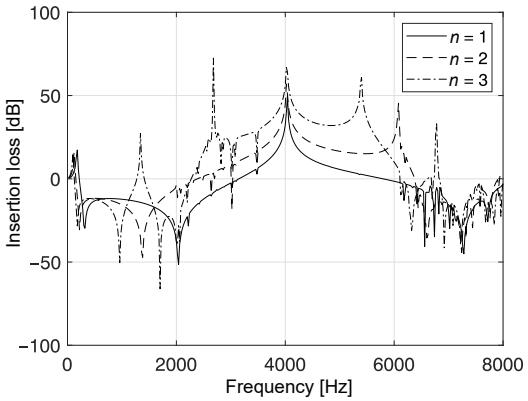

Fig. 2. IL as a function of number of scatterer rows in DPS.

The widths of frequency range where the IL is larger than zero are 2660 Hz, 3980 Hz, and 3820 Hz. And the widths for number of 2 and 3 are about the same.

Figure 3 shows the STL through the DPS for the number of scatterer rows of 2. The sound insulation, added the effect of two panels, exhibits a high transmission loss (TL) of larger than 80 dB in a broad frequency range from 2360 Hz to 6540 Hz, even though the number of scatterer rows is 2. It is therefore obvious that two rows of scatterers are enough to give a sufficiently wide and high band gap around the Bragg frequency in DPS.

Next, the maximum TL and width of the Bragg-type band gap are evaluated with varying the filling fraction from 10% to 70% through the outer radius of the 2 rows of cylindrical scatterers (Figs. 4 and 5).

For the filling fraction of larger than 10%, the peak of the IL increases slowly giving a relatively small

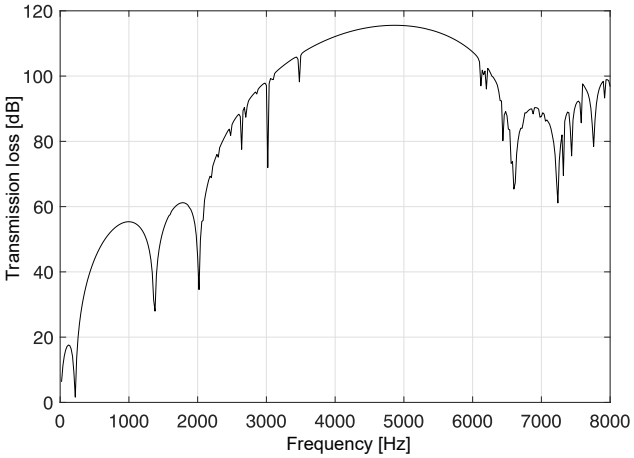

Fig. 3. STL of DPS with 7×2 cylindrical scatterers arranged on square lattice.

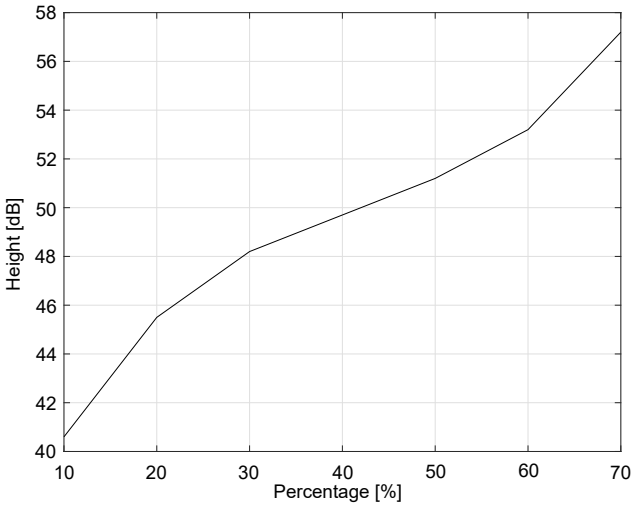

Fig. 4. Peak of IL as a function of filling fraction.

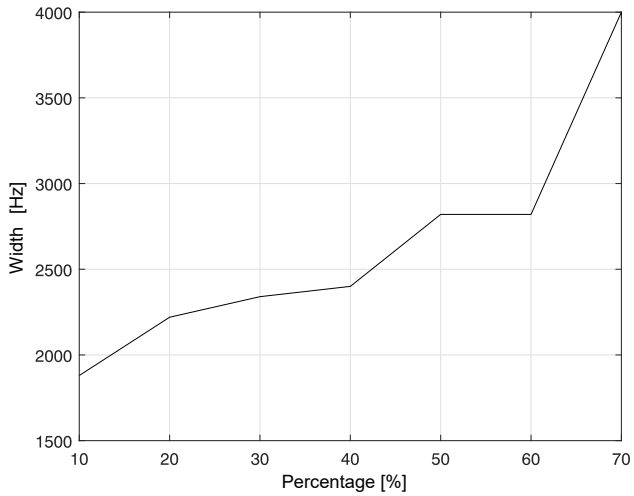

Fig. 5. Width of insertion loss peak as a function of filling fraction.

steepness. The variation of the peak is about 10–14 dB in the entire range of filling fraction from 10% to 70%.

Besides, it can be found from Fig. 5 that the width of frequency range where the IL is larger than zero does not change remarkably for the filling fraction from 10% to 60%. However, it increases rapidly for the filling fraction larger than 60%. As a result of this, it can be concluded that the effect of the filling fraction on the Bragg-type band gap is relatively weak.

3.2. Effects of local resonances

Since an array of elastic shells exposed to the environment would not be practical for an outdoor noise barrier, protecting the shells using concentric outer PVC cylinders offers a simple solution. However, for those inserted between two panels, there is no such problem.

The ring-type shells are considered to be made of commercially available non-vulcanized rubber, of which the material properties are the density of ρ = 1100 kg/m^3, the Young's modulus of E = 1.75 MPa, and the Poisson's ratio of ν = 0.4997. The outer diameter and thickness of the ring shells are 40 mm and 0.5 mm, respectively. Spacing between neighboring scatterers is 42.8 mm and they are arranged on 7×3 square lattice.

Figure 6 shows STL through the DPS with three rows of the thin ring shells.

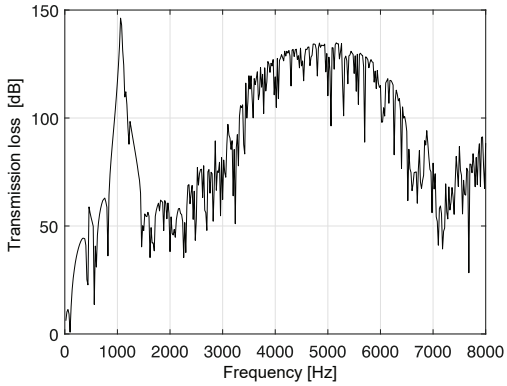

Fig. 6. STL through DPS with a ring-type scatterer array.

The curve has a very high band gap around the low frequency, 1060 Hz, as well as a Bragg-type band gap caused by the periodicity of the lattice, which is attributed to the local resonance of the ring-type scatterers. Meanwhile, TLs in the Bragg band gap fluctuate constantly. This might be due to the variation of the outer diameter caused by the breathing vibration of the scatterers. Fluctuating the outer diameter of the scatterers follows by one of the filling fraction, resulting in the following variation of the sound performance of the SCs.

Figure 7 shows the IL spectra for the solid cylinder array and the ring-type scatterers. As shown in the figure, unlike the case of cylindrical scatterers, there exists a band gap of very large ILs (78 dB) at low frequencies (center frequency of 1020 Hz, width of 600 Hz) attributed to the local breathing-type resonance for the ring scatterers.

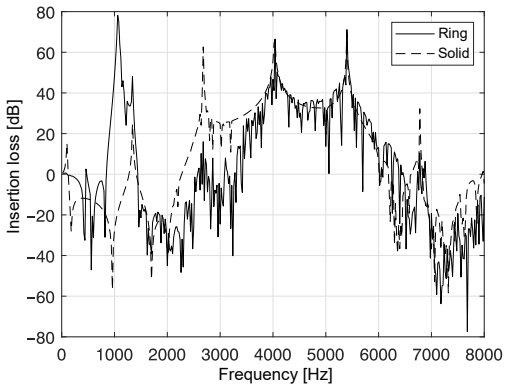

Fig. 7. IL spectra for solid cylinder arrays and ring-type scatterers.

Figure 8 shows the IL for SC consisted of the cylindrical scatterers compared to one for the Helmholtz resonant scatterers. Helmholtz resonators have the outer diameter of 35 mm, the thickness of 1.5 mm, and the slit width of 14 mm. They are assumed to be made of the same plastic as two panels.

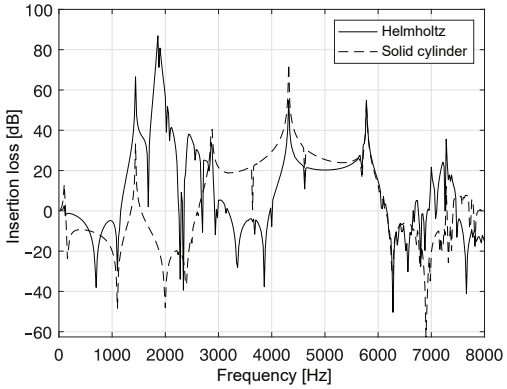

Fig. 8. ILs for solid cylindrical scatterers versus Helmholtz resonant scatterers.

Two ILs at the Bragg frequency are approximately comparable with each other. However, Helmholtz resonator array gives the IL higher than that for the cylindrical scatterer array at the stand wave resonance frequencies as in 1400 Hz. It is also the same at the local resonance frequencies.

3.3. Combination effect of breathing resonance and Helmholtz resonance

Coupling the local resonances in the individual scatterers enables the sound insulation in a certain frequency range to be enhanced. From Eq. (9), it is necessary to increase the thickness or the diameter of the scatterers in order to decrease the resonance frequency of SRRs. This results in the thicker and more weighted construction for soundproofing.

On the other hand, as shown in Figs. 6 and 7, the thin ring scatterer exhibits a very high local resonant band gap. And because the ring scatterers are very thin and made of the materials with a relatively small density, they are lighter than the Helmholtz resonators with the same outer diameter. For example, the mass per length of a Helmholtz resonator used above is about 250 g, while one of a ring scatterer is 68 g, lighter by a factor of about 3.6. If the Helmholtz resonators were made of metallic material rather than plastic, the mass difference would become larger. Thus, coupling the two kind of resonators would not only create the several local resonant band gaps at low frequencies, but also reduce markedly the total weight of the soundproofing structure.

Figure 9 shows the schematic and STL of a DPS with one row of Helmholtz resonators, of which the outer diameter is 35 mm, the thickness 1.5 mm, and the slit width 14 mm, and two rows of ring scatterers, of which the outer diameter is 35 mm and the thickness 0.5 mm. The STL for the DPS filled with air between two panels is also plotted in the figure.

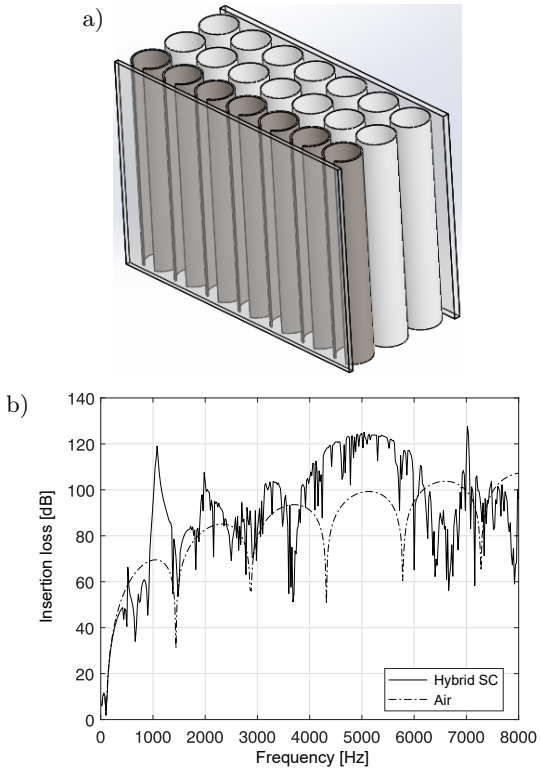

Fig. 9. Schematic (a) and STL (b) of DPS with 7×3 hybrid SC and filled with air.

In the TL curve, there exist very high peaks at the frequencies of 1080, 1440, 1980, and 2860 Hz below the Bragg-type band gap. The peaks at 1080 Hz and 1980 Hz are attributed to the breathing-type resonance of ring scatterers and Helmholtz resonance of SRR, while the other peaks are caused by the suppressions of stand wave resonances. These two types of resonances improve the sound insulation in the frequency range from 1000 Hz to 2300 Hz by an average of 13 dB compared to that without the hybrid SC, with a maximum of 50 dB.

Figure 10 shows the STLs for one row versus two rows of ring scatterers (solid line in Fig. 9b).

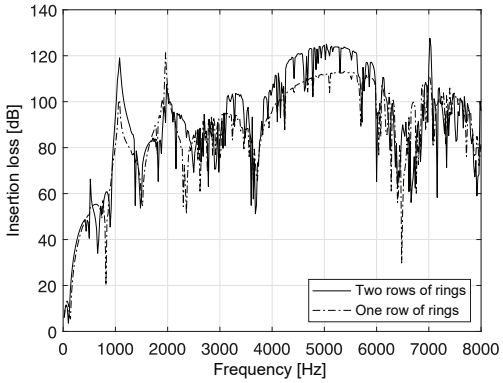

Fig. 10. STLs through DPSs with 7×2 and 7×3 hybrid SCs.

It can be seen from the figure that when the total number of scatterer rows decreases from three to two, the maximum TL of the Bragg band gap was reduced by 8 dB, and the maximum TL of the resonant band gap at the breathing resonance frequency was also reduced by a few dB due to a reduction in the number of ring resonator rows. However, the sound insulation performances in the other frequency ranges are almost similar, and the position and width of the Bragg band gap are also unchanged. In addition, even when the number of ring scatterer rows is 1, the maximum TLs of both the Bragg band gap and the resonant band gap at the breathing resonance frequency are higher than 100 dB. At the same time, the total thickness of DPS decreased by 40 mm from 130 to 90 mm as the scatterer decreased by one.

It can be concluded that combining the two resonances can improve the low-frequency sound insulation, reduce the mass and volume of the entire structure as well as SC.

3.4. Combination effect of porous material and hybrid local resonant SC

Figures 11 and 12 show the effect of porous material (glass wool) on the sound insulation of DPS with the hybrid SC as in Fig. 9 through the STL and IL. As shown in Fig. 11, inserting the porous material leads to the elimination of the deep dips in the STL spectrum due to the two kinds of local resonant scatterer arrays, a significant increase in the soundproofing performance in the overall frequency range, and a relatively smooth TL over 60 dB in the frequency range above 1 kHz. Figure 11 also shows TL through the DPS filled only with glass wool (without hybrid SC)

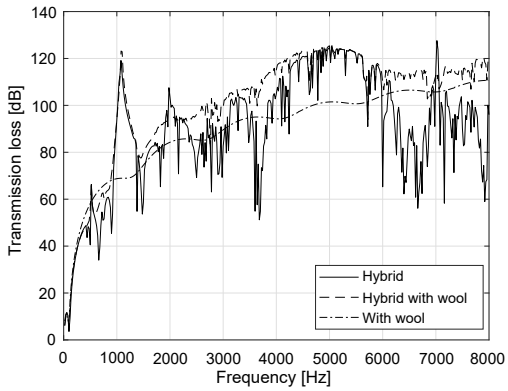

Fig. 11. STLs of DPSs with hybrid SC embedded in porous material or without it.

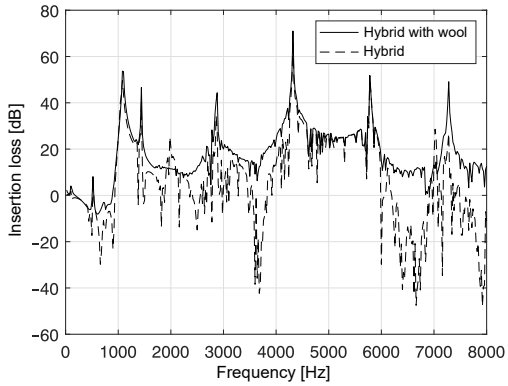

Fig. 12. ILs in DPSs with hybrid SC embedded in porous material and without it.

(dashed dotted line). It can be seen that the sound insulation is improved by more than 15 dB on average in the frequency range above 1 kHz compared with DPS only with glass wool.

These tendencies can be seen in Fig. 12, and by filling with the glass wool, the insertion loss at almost all frequencies is greater than zero. Therefore, in order to enhance sound insulation of DPS only in a particular low frequency range, a hybrid local resonator array with appropriate resonant frequencies should be inserted in two panels of the DPS, while in the case of high insulation performance in the whole frequency range, SCs and porous materials must be combined together.

4. Conclusions

In this paper, a new approach was proposed to reduce the size and mass of DPS while improving the acoustic insulation performance by using the SC coupled with two kinds of local resonance effects. It is found that the minimum number of scatterer rows to form a broad and high forbidden band at the Bragg frequency is two and the filling fraction has relatively little effect on the Bragg band gap in the DPS. In addition, combining the resonances of Helmholtz resonators with the breathing resonances of ring scatterers can not only reduce the thickness and mass of DPS, but also create several resonant band gaps at low frequencies. Also, when the local resonant SCs are applied to DPS, the use of porous materials together can lead to a relatively smooth and high forbidden band around the resonance frequencies. It also provides about 15 dB higher sound insulation than DPS only with glass wool in the frequency range above 1 kHz.

Acknowledgments

The authors wish to thank the anonymous reviewers for their valuable comments, constructive remarks, and suggestions to improve the quality of the paper.

References

1. Bies D.A., Hansen C.H. (1980), Flow resistance information for acoustical design, *Applied Acoustics*, **13**(5): 357–391, doi: 10.1016/0003-682X(80)90002-X.
2. Brillouin L. (1946), *Wave Propagation in Periodic Structures*, 2nd ed., Dover Publications Inc.
3. Cavalieri T., Cebrecos A., Groby J.-P., Chaufour C., Romero-García V. (2019), Three-dimensional multiresonant lossy sonic crystal for broadband acoustic attenuation: Application to train noise reduction, *Applied Acoustics*, **146**: 1–8, doi: 10.1016/j.apacoust.2018.10.020.
4. Chalmers L., Elford D.P., Kusmartsev F.V., Swallowe G.M. (2009), Acoustic band gap formation in two-dimensional locally resonant sonic crystals comprised of Helmholtz resonators, *International Journal of Modern Physics B*, **23**(20n21): 4234–4243, doi: 10.1142/S0217979209063390.
5. Chen Y.-Y., Ye Z. (2001), Theoretical analysis of acoustic bands in two-dimensional periodic arrays, *Physical Review E*, **64**: 036616, doi: 10.1103/PhysRevE.64.036616.
6. Delany M.E., Bazley E.N. (1970), Acoustical properties of fibrous absorbent materials, *Applied Acoustics*, **3**: 105–116, doi: 10.1016/0003-682X(70)90031-9.
7. Elford D.P., Chalmers L., Kusmartsev F.V., Swallowe G.M. (2011), Matryoshka locally resonant sonic crystal, *The Journal of the Acoustical Society of America*, **130**(5): 2746–2755, doi: 10.1121/1.3643818.
8. Fuster-Garcia E., Romero-García V., Sánchez-Pérez J.V., García-Raffi L.M. (2007), Targeted band gap creation using mixed sonic crystal arrays including resonators and rigid scatterers, *Applied Physics Letter*, **90**(24): 244104, doi: 10.1063/1.2748853.
9. Gulia P., Gupta A. (2018), Enhancing the sound transmission loss through acoustic double panel using sonic crystal and porous material, *The Journal of the Acoustical Society of America*, **144**(3): 1435–1442, doi: 10.1121/1.5054296.

10. Gulia P., Gupta A. (2019), Sound attenuation in triple panel using locally resonant sonic crystal and porous material, *Applied Acoustics*, **156**: 113–119, doi: 10.1016/j.apacoust.2019.07.012.

11. Hirsekorn M., Delsanto P.P., Batra N.K., Matic P. (2004), Modelling and simulation of acoustic wave propagation in locally resonant sonic materials, *Ultrasonics*, **42**(1–9): 231–235, doi: 10.1016/j.ultras.2004.01.014.

12. Kim M.-J. (2019), Numerical study for increasement of low frequency sound insulation of double-panel structure using sonic crystals with distributed Helmholtz resonators, *International Journal of Modern Physics B*, **33**(14): 1950138, doi: 10.1142/S0217979219501388.

13. Kim M.-J., Rim C.-G., Won K.-S. (2021), Broadening low-frequency band gap of double-panel structure using locally resonant sonic crystal comprised of slot-type Helmholtz resonators, *Archives of Acoustics*, **46**(2): 335–340, doi: 10.24425/aoa.2021.136587.

14. Kyrnkin A., Umnova O., Chong Y.B.A., Taherzadeh S., Attenborough K. (2010), Predictions and measurements of sound transmission through a periodic array of elastic shells in air, *The Journal of the Acoustical Society of America*, **128**(6): 3496–3506, doi: 10.1121/1.3506342.

15. Linton C.M., Evans D.V. (1990), The interaction of waves with arrays of vertical circular cylinders, *Journal of Fluid Mechanics*, **215**: 549–569, doi: 10.1017/S0022112090002750.

16. Martínez-Sala R., Rubio C., Garcia-Raffi L.M., Sánchez-Pérez J.V., Sánchez-Pérez E.A., Llinares J. (2006), Control of noise by trees arranged like sonic crystals, *Journal of Sound and Vibration*, **291**(1–2): 100–106, doi: 10.1016/j.jsv.2005.05.030.

17. Martínez-Sala R., Sancho J., Sánchez J.V., Gómez V., Llinares J., Meseguer F. (1995), Sound attenuation by sculpture, *Nature*, **378**: 241, doi: 10.1038/378241a0.

18. Movchan A.B., Guenneau S. (2004), Split-ring resonators and localized modes, *Physical Review B*, **70**: 125116, doi: 10.1103/PhysRevB.70.125116.

19. Qian D. (2018), Wave propagation in a LRPC composite double panel structure with periodically attached pillars and etched holes, *Archives of Acoustics*, **43**(4): 717–725, doi: 10.24425/aoa.2018.125165.

20. Romero-García V., Garcia-Raffi L.M., Sánchez-Perez J.V. (2011), Evanescent waves and deaf bands in sonic crystals, *American Institute of Physics Advances*, **1**: 041601, doi: 10.1063/1.3675801.

21. Sainidou R., Djafari-Rouhani B., Pennec Y., Vasseur J.O. (2006), Locally resonant phononic crystals made of hollow spheres or cylinders, *Physical Review B*, **73**(2): 024302, doi: 10.1103/PhysRevB.73.024302.

22. Sánchez-Dehesa J., Garcia-Chocano V.M., Torrent D., Cervera F., Cabrera S. (2011), Noise control by sonic crystal barriers made of recycled material, *The Journal of the Acoustical Society of America*, **129**(3): 1173–1183, doi: 10.1121/1.3531815.

23. Sanchez-Perez J.V., Rubio C., Martinez-Sala R., Sanchez-Grandia R., Gomez V. (2002), Acoustic barriers based on periodic arrays of scatterers, *Applied Physics Letters*, **81**: 5240–5242, doi: 10.1063/1.1533112.

24. Sohn C.H., Park J.H. (2011), A comparative study on acoustic damping induced by half-wave, quarter-wave and Helmholtz resonators, *Aerospace Science and Technology*, **15**(8): 606–614, doi: 10.1016/j.ast.2010.12.004.

25. Umnova O., Attenborough K., Linton C.M. (2006), Effects of porous covering on sound attenuation by periodic arrays of cylinders, *The Journal of the Acoustical Society of America*, **119**(1): 278–284, doi: 10.1121/1.2133715.

26. Vasseur J.O., Deymier P.A., Djafari-Rouhani B., Pennec Y., Hladky-Hennion A-C. (2008), Absolute forbidden bands and waveguiding in two-dimensional phononic crystal plates, *Physical Review B*, **77**(8): 085415, doi: 10.1103/PhysRevB.77.085415.

27. Wu L.-Y., Chen L.-W., Wu M.-L. (2008), The nondiffractive wave propagation in the sonic crystal consisting of rectangular rods with a slit, *Journal of Physics: Condensed Matter*, **20**: 295229, doi: 10.1088/0953-8984/20/29/295229.